

## Rapid detection of cardiac troponin I using antibody-immobilized gate-pulsed AlGaIn/GaN high electron mobility transistor structures

Jiancheng Yang, Patrick Carey, Fan Ren, Yu-Lin Wang, Michael L. Good, Soohwan Jang, Michael A. Mastro, and S. J. Pearton

Citation: [Appl. Phys. Lett.](#) **111**, 202104 (2017);

View online: <https://doi.org/10.1063/1.5011151>

View Table of Contents: <http://aip.scitation.org/toc/apl/111/20>

Published by the [American Institute of Physics](#)

---

### Articles you may be interested in

[Large-area SnSe<sub>2</sub>/GaN heterojunction diodes grown by molecular beam epitaxy](#)

*Applied Physics Letters* **111**, 202101 (2017); 10.1063/1.4994582

[BInGaIn alloys nearly lattice-matched to GaN for high-power high-efficiency visible LEDs](#)

*Applied Physics Letters* **111**, 211107 (2017); 10.1063/1.4997601

[Unidirectional ultraviolet whispering gallery mode lasing from floating asymmetric circle GaN microdisk](#)

*Applied Physics Letters* **111**, 202103 (2017); 10.1063/1.4991570

[Degradation of 2DEG transport properties in GaN-capped AlGaIn/GaN heterostructures at 600 °C in oxidizing and inert environments](#)

*Journal of Applied Physics* **122**, 195102 (2017); 10.1063/1.5011178

[Asymmetrical quantum well degradation of InGaIn/GaN blue laser diodes characterized by photoluminescence](#)

*Applied Physics Letters* **111**, 212102 (2017); 10.1063/1.5001372

[High-performance solar-blind Al<sub>0.6</sub>Ga<sub>0.4</sub>N/Al<sub>0.5</sub>Ga<sub>0.5</sub>N MSM type photodetector](#)

*Applied Physics Letters* **111**, 191103 (2017); 10.1063/1.5001979

---



# SciLight

Sharp, quick summaries **illuminating**  
the latest physics research

Sign up for **FREE!**

**AIP**  
Publishing

# Rapid detection of cardiac troponin I using antibody-immobilized gate-pulsed AlGaIn/GaN high electron mobility transistor structures

Jiancheng Yang,<sup>1</sup> Patrick Carey IV,<sup>1</sup> Fan Ren,<sup>1</sup> Yu-Lin Wang,<sup>2</sup> Michael L. Good,<sup>3</sup> Soohwan Jang,<sup>4</sup> Michael A. Mastro,<sup>5</sup> and S. J. Pearton<sup>6</sup>

<sup>1</sup>Department of Chemical Engineering, University of Florida, Gainesville Florida 32611, USA

<sup>2</sup>Institute of Nanoengineering and Microsystems and Department of Power Mechanical Engineering, National Tsing Hua University, Hsinchu 300, Taiwan

<sup>3</sup>Department of Anesthesiology, College of Medicine, University of Florida, Gainesville, Florida 32611, USA

<sup>4</sup>Department of Chemical Engineering, Dankook University, Yongin 16890, South Korea

<sup>5</sup>U.S. Naval Research Laboratory, Washington, DC 20375, USA

<sup>6</sup>Department of Materials Science and Engineering, University of Florida, Gainesville, Florida 32611, USA

(Received 30 October 2017; accepted 7 November 2017; published online 17 November 2017)

We report a comparison of two different approaches to detecting cardiac troponin I (cTnI) using antibody-functionalized AlGaIn/GaN High Electron Mobility Transistors (HEMTs). If the solution containing the biomarker has high ionic strength, there can be difficulty in detection due to charge-screening effects. To overcome this, in the first approach, we used a recently developed method involving pulsed biases applied between a separate functionalized electrode and the gate of the HEMT. The resulting electrical double layer produces charge changes which are correlated with the concentration of the cTnI biomarker. The second approach fabricates the sensing area on a glass slide, and the pulsed gate signal is externally connected to the nitride HEMT. This produces a larger integrated change in charge and can be used over a broader range of concentrations without suffering from charge-screening effects. Both approaches can detect cTnI at levels down to 0.01 ng/ml. The glass slide approach is attractive for inexpensive cartridge-type sensors. *Published by AIP Publishing.*  
<https://doi.org/10.1063/1.5011151>

Cardiac troponin I (cTnI) and the complex involving cTnI, cardiac troponin T (cTnT), and cardiac troponin C (cTnC) in the cardiac muscle tissue are the standard clinical biomarkers for acute myocardial infarction (AMI) and diseases that produce cardiac muscle damage.<sup>1–15</sup> The concentrations of these species rise quickly in the blood following the onset of AMI as they are released from myocardial cells following cell death.<sup>1,2,8,16,17</sup> Elevated troponin concentrations can be detected in the blood within a few hours up to several days following the onset of angina (where myocardial cells suffer reversible damage) to AMI where myocardial cells die.<sup>10,14–17</sup> The time-dependence of the concentration of these species is commonly detected by antigen-antibody or aptamer-based interactions using techniques such as radioimmunoassay, enzyme-linked immunosorbent assay (ELISA), fluorimetric, luminometric, colorimetric, and amperometric (electrochemical) methods.<sup>14–17</sup> Many of these are time consuming and require trained personnel to perform tests.<sup>2,10,15</sup> The challenge is to develop a real-time, accurate, handheld, and low cost heart attack sensor.<sup>14–17</sup> The measurement of blood troponin concentrations can decide whether AMI has occurred or chest pain and other symptoms are due to other causes.<sup>1,15</sup> Inexpensive techniques that provide rapid, accurate blood troponin concentrations would be welcome in managing the treatment of patients in emergency room situations.

Field-effect transistors (FETs) functionalized with antibodies or aptamer layers in the gate region, often referred to as bio-FETs, can be effective sensors for a variety of biomarkers.<sup>18–25</sup> In particular, AlGaIn/GaN high electron mobility transistors (HEMTs) are an attractive option.<sup>18,20,21,26,27</sup> Due to spontaneous and piezoelectric polarization, a two dimensional electron gas (2DEG) channel exists at the

interface between AlGaIn and GaN, and the carrier conductivity at the 2DEG channel is very sensitive to surface charge changes in the gate region.<sup>18,27</sup> Typically, HEMTs with a higher channel conductivity show a better sensitivity for biomarker detection. With the 30% Al concentration in the AlGaIn layer, 5–10 times higher sheet electron densities are obtained compared to GaAs or InP HEMTs.<sup>18</sup> Also, the intrinsic carrier concentration of GaN is  $10^{-10} \text{ cm}^{-3}$ , while that of Si is  $10^{10} \text{ cm}^{-3}$ , which enables stable operation of the sensor at higher temperatures. Lee *et al.*<sup>25</sup> showed that improved detection limits can be obtained with differential-mode HEMT biosensors employing an Au-gate HEMT as the sensing device to react with biomolecules, while a separate Pt-gate HEMT is the dummy device in the differential-mode detection circuit. Both the biosensing HEMT and reference HEMT are biased by a Pt quasi-reference electrode. Sarangadharan *et al.*<sup>26</sup> reported an electrical double layer gated high field AlGaIn/GaN HEMT biosensor in which the gating mechanism overcomes charge screening effects that are prevalent in traditional FET based biosensors, allowing detection of target proteins in physiological solutions. They were able to detect troponin I in blood samples at low concentrations and in the wide dynamic range (0.006–148 ng/ml), using both antibody and aptamer functionalization.<sup>26</sup> In this design, when the gate electrode is positively biased, negative ions accumulate on the surface of the open area on the gate electrode. Similarly, positive ions accumulate on the open area of the channel, resulting in an increased carrier density in the 2DEG.<sup>26,27</sup> An electronic double layer forms on the gate metal and the surface of the channel. Introduction of a solution on the top of the HEMT changes the capacitance of the effective gate dielectric, and if this capacitance changes due to binding

reactions, the voltage in solution drops and the gate voltage also changes, resulting in a change in drain current.<sup>26,27</sup>

In this paper, we report an investigation of two testing techniques using AlGaIn/GaN HEMTs to detect cTnI. For the conventional or dipping sensor, the gate electrode area is electrically connected to a nearby area functionalized with the troponin antibody. This functionalized electrode is spaced apart from the gate of the HEMT, with the biomarker introduced into contact with the gate and the reactive electrode.<sup>27</sup> A pulsed voltage is applied between the reactive electrode and the source, and the resulting current is recorded. In the second approach, we use a HEMT connected to a cover glass with functionalized and reference areas. The functionalized area is again subjected to voltage pulses, while the reference area is connected to the gate of the HEMT. Then, bias pulses are applied to the gate side and the drain terminal, and the total accumulated charge is calculated from the monitored response current. This voltage pulsing changes the ion distribution in the solution and leads to changes in drain current.<sup>26–28</sup> We show that the latter approach is advantageous in providing a larger current and charge change for detection and for being more versatile in terms of miniaturized sensor designs.

The AlGaIn/GaN HEMT structures were grown on AlN low temperature layers on c-axis sapphire substrates with 2.2  $\mu\text{m}$  of undoped GaN and 25 nm of  $\text{Al}_{0.25}\text{Ga}_{0.75}\text{N}$  by metal organic chemical vapor deposition. Inductively coupled plasma (ICP) etching was used to remove 110 nm of material for

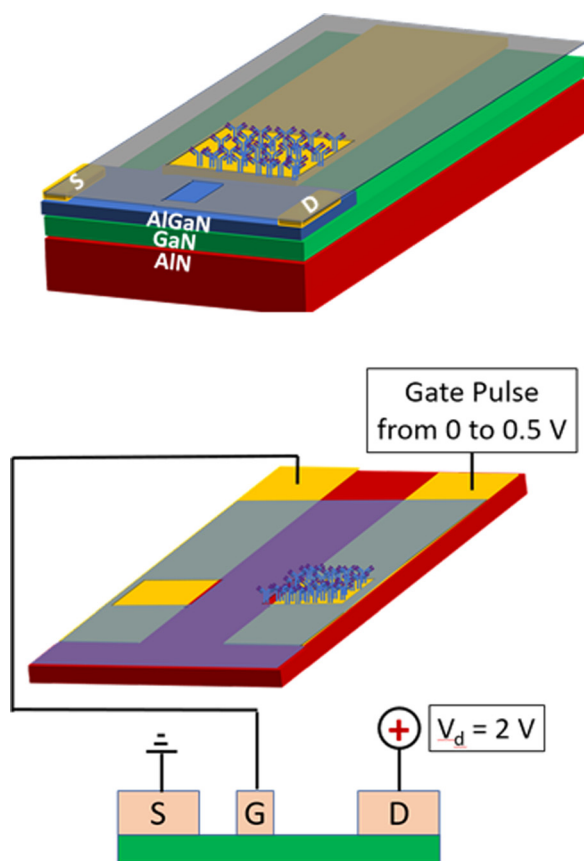


FIG. 1. Schematic of the “dipping” sensor, containing a functionalized area on the channel placed at a small distance from the gate electrode (bottom). Schematic of the cover glass approach after functionalization, and the connections between cover glass and the FET device. The gate is again pulsed from 0 to 2 V, while the drain voltage is 2 V.

device isolation [ $\text{Cl}_2/\text{Ar}$ , 200 W (2 MHz) source power, 50 W RF (13.56 MHz) chuck power at 5 mTorr, and  $\sim 150$  V DC bias voltage on the chuck electrode]. The source and drain Ohmic contact pads were metalized by lift-off of E-beam evaporated Ti/Al/Ni/Au (25/125/45/100 nm) and then annealed at 850  $^{\circ}\text{C}$  for 45 s in  $\text{N}_2$ . Source, drain, and gate electrodes were patterned by lift-off of Ti/Au (20/80 nm).

To perform the surface functionalization of the first design in which the functional layer is on the HEMT itself, a 100 nm  $\text{SiN}_x$  passivation layer was deposited on the entire wafer. A square opening ( $100 \times 120 \mu\text{m}$ ) on the gate electrode and the active gate channel area ( $10 \times 50 \mu\text{m}$ ) 30  $\mu\text{m}$  apart were opened using lithography. To immobilize the Anti-Cardiac Troponin I antibody, thioglycolic acid (TGA,  $\text{HSCH}_2\text{COOH}$ ) was used as a binding agent between the gold surface and the antibody molecule. The gate electrode was exposed to TGA solution for functionalization. The sample surface was treated with Ozone (10 min) to remove carbon contamination on the exposed Au surface before thioglycolic acid treatment.<sup>18</sup> We have shown previously that this process leads to complete coverage of the semiconductor surface through X-Ray Photoelectron Spectroscopy that showed the formation of thiolated S–Au bonds<sup>29</sup> and current-voltage measurements after functionalization which no longer showed a response to the

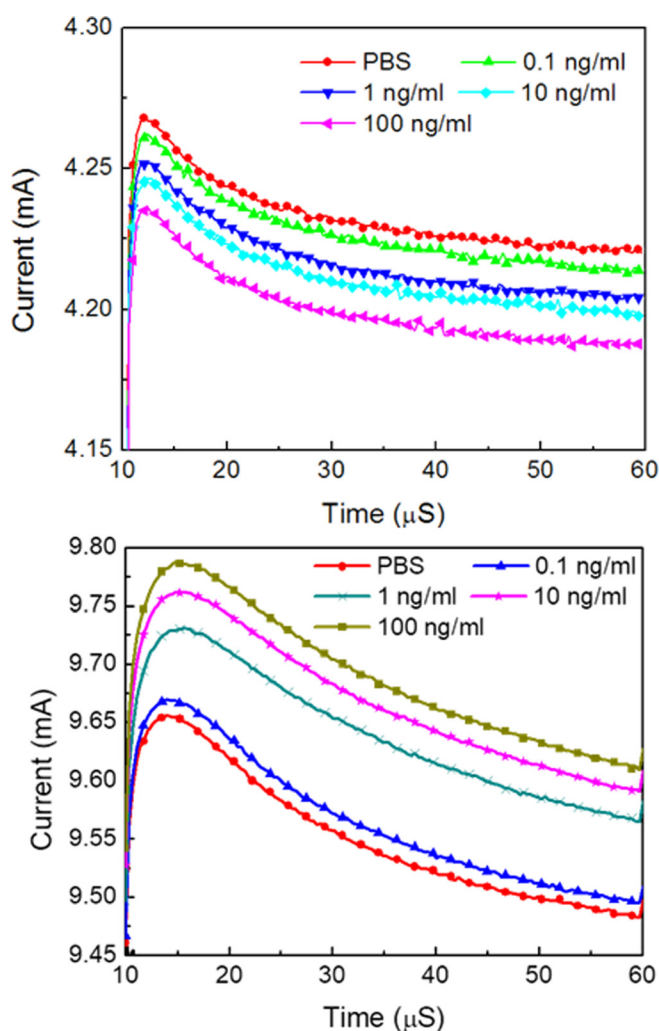


FIG. 2. Drain current response with different cTnI concentrations using either the dipping sensor (top) or cover glass (bottom) approaches.

TABLE I. Summary of changes in current for different concentrations of Troponin I protein in  $1 \times$  PBS with 1% BSA.

	Conventional (dipping) sensor	Cover plate sensor
CtNI concentration (ng/ml)	$\Delta I$ ( $\mu$ A); total charge (nC)	$\Delta I$ ( $\mu$ A); total charge (nC)
0 (PBS)	0; 210.1	0; 478.0
0.1	-8.6; 209.7	14.6; 478.8
1	-19.4; 209.3	87.8; 482.5
10	-25.3; 209.0	116.2; 483.9
100	-36.7; 208.5	137.7; 485.0

addition of water to the gate region, indicating that the entire gate area was covered by thiols that blocked ions from Au.<sup>30</sup> Then, the lithographically exposed gate electrode was functionalized with 1 mM of TGA solution for 12 h. The TGA side group and the thiol group strongly interact with and bond to Au and self-assemble to form a TGA monolayer on Au, and exposure of the carboxylic group (another TGA side group) produces a further chemical linking reaction to the antibodies. The wafer was rinsed with de-ionized wafer to remove excess TGA and then with acetone to strip the resist. The Anti-Cardiac Troponin I antibody (100  $\mu$ g/ml) was introduced to the wafer surface, and the sample was stored at 4 °C for three hours to immobilize the antibody. The wafer was rinsed with 10 mM PBS solution to remove the un-bonded antibody from the wafer surface. Figure 1 (top) shows a schematic after functionalization of this more conventional approach, which we call a dipping sensor.

The second design, labelled the cover glass approach, differs by incorporating the formation of Schottky contacts

by E-beam deposition of Ni/Au (20 nm/80 nm). On the cover glass, separated (20  $\mu$ m separation) metal lines (Ni/Au; 20 nm/80 nm) were formed by lithography and E-beam deposition. Only one of the openings on the cover glass was functionalized with the antibody, while the other was a reference. Figure 1 (bottom) shows the schematic of this approach.

For detection of cTnI, drain currents were measured at 25 °C using an Agilent B1500 parameter analyzer with Be/Cu probe tips. The Agilent B1530 pulse generator was also used to generate a step waveform function for both gate and drain electrodes, with a delay period of 8  $\mu$ s for both pulse signals. The HEMTs were biased with 2 V on the drain and with 0 V on the gate for 2  $\mu$ s. Then, 0.5 V was applied to the gate for 50  $\mu$ s while keeping the drain bias at 2 V. Once the gate voltage dropped to 0 V, the drain was biased for extra 5  $\mu$ s before it dropped to 0 V. The rise and fall time for each pulse function was  $\sim$ 80 ns. The targeted Natural Cardiac Troponin I protein concentrations were 0.1  $\mu$ g/ml, 1  $\mu$ g/ml, 10  $\mu$ g/ml, and 100 ng/ml in  $1 \times$  PBS with 1% BSA (Table I). The level of cTnI in AMI patients is around 10 ng/ml and can go up to 10–550 ng/ml. For early detection of AMI patients, the cTnI concentration is in the range of 0.5–2.0 ng/ml. Before each measurement for individual target concentrations, there was five minutes of the buffering time for the Natural Cardiac Troponin I protein to bind to the Anti-Cardiac Troponin I antibody. The cover glass approach employed the same 2 V bias on the drain, with the gate electrode connected to the un-functionalized Au electrode. The functionalized side of the gold electrode was connected to the pulse generator. The functionalized side of the gold electrode is labelled the cover glass active electrode. The pulse generator produced a step waveform function for both cover

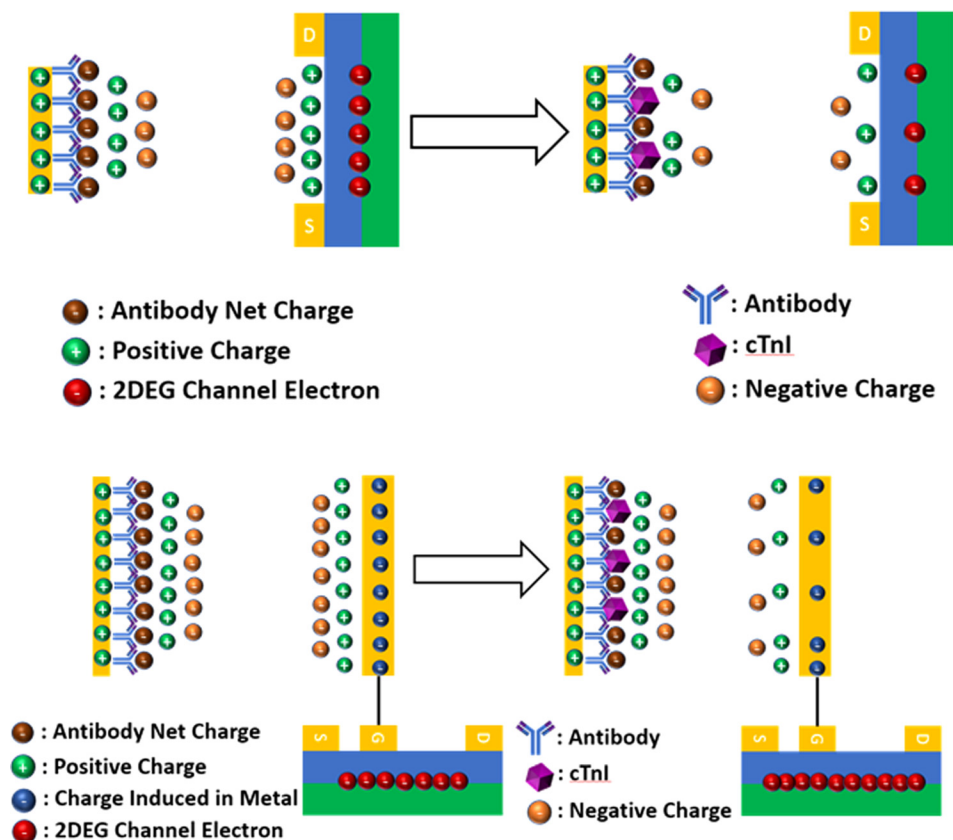


FIG. 3. Schematic of charge and current changes as a result of antigen-antibody binding in the two types of sensors.

glass active and drain electrodes. There was the same 8  $\mu$ s delay period for both pulse signals, and then, the HEMT was biased at the 2 V drain electrode and 0 V to the cover glass active electrode for 2  $\mu$ s. Then, 0.5 V of voltage was applied to the cover glass active electrode for 50  $\mu$ s while keeping the drain biased voltage at 2 V. Once after the cover glass active biased voltage dropped to 0 V, the drain electrode was biased for extra 5  $\mu$ s before it was reduced to 0 V. Five devices of each type were tested, and each data point represents the average of three measurements from each of these devices.

Figure 2 (top) shows the drain current characteristics of the conventional dipping sensor with different troponin concentrations. The troponin causes a decrease in current relative to standard PBS solution, as reported previously.<sup>26</sup> The analysis of the electrical double layer formed during the pulsed biasing of functionalized HEMTs has also been covered in detail previously.<sup>27</sup> By contrast, the cover glass approach leads to an increase in the pulsed current, as shown in Fig. 2 (bottom). In this configuration, the receptor immobilization produces a decrease in the total capacitance of the solution plus dielectric capacitance and thus a decrease in effective gate voltage and an increase in current.<sup>26</sup> The larger change in the signal from the glass sensor results from the higher fall-off of field and higher charge induced on the AlGaIn surface in this configuration, as shown schematically in Fig. 3. The sign of the current change depends on field distribution, ion mobility, relaxation times, and concentration, and the integrated current (i.e., the charge) is a superior measure of biosensor response.<sup>28</sup>

The sensing mechanism is binding of the antibody to the receptor, which can be assumed to be a reversible reaction whose dissociation constant follows a one site binding model.<sup>26</sup> In Fig. 4, we show the experimental values of current change and fits to the one site model. The model fitting for this set of data is based on the Langmuir Extension model with

$$\Delta I = \frac{a * b * [C]^{(1-d)}}{1 + b * [C]^{(1-d)}},$$

where  $\Delta I$  is the change in drain current ( $\mu$ A),  $[C]$  is the antigen concentration (ng/ml), and  $a$ ,  $b$ , and  $d$  are constants. The model fitting for this dataset produced the following relations:

$$\Delta I = \frac{14.14 * [C]^{0.29}}{1 + 0.14 * [C]^{0.29}}$$

for the dipping sensor and

$$\Delta I = \frac{184 * [C]^{1.08}}{1 + 1.84 * [C]^{1.08}}$$

for the cover glass sensor. The good fits to the experimental data show that the one site approximation is reasonable in this case. The 5% error bars in Fig. 4 result from the uncertainty in drain current at 0.5 V gate pulsed voltage measured between different concentrations of the antigen and PBS. The errors are around 6 and 7.5  $\mu$ A in Fig. 4 (top) and (bottom), respectively.

As reported by Sarangadharan *et al.*<sup>26</sup> and Hsu *et al.*,<sup>28</sup> the sensitivity can be enhanced and effects of random noise can be reduced by calculating the total charge accumulated on the HEMT surface by integrating the drain current over time. Since the change in current as a result of antigen-

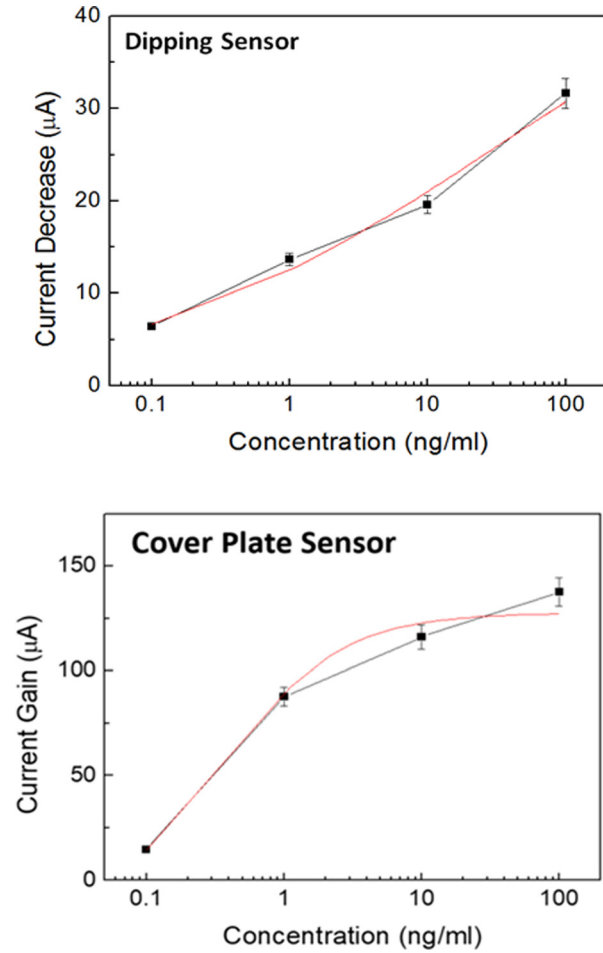


FIG. 4. Change in current (data points) for different concentrations of Troponin I protein in  $1 \times$  PBS with 1% BSA for the dipping sensor (top) or the cover glass sensor (bottom). Also shown is the fit to the Langmuir extension model.

antibody binding is related to the time rate of change of charge, i.e.,  $I = \frac{\partial Q}{\partial t}$ , we can calculate the total charge by the integration of the current curve from the drain current response to different Troponin I concentrations. The PBS data point is not included in this figure because it is plotted in a semi-log scale. In Fig. 5, we plot the total charges passing through the 2DEG within 50  $\mu$ s. Since the drain current of these two setups is 4.5 and 9.7 mA, respectively, the percent errors caused by 6 and 7.5  $\mu$ A are very small in total charges, corresponding to errors of 0.01% and 0.008%, respectively. The charge variations shown in Fig. 5 are approximately in proportion to the logarithmic biomarker concentration in the liquid sample. The charge accumulated at the biosensor within a pulse width of an applied voltage pulse can be correlated with the analyte concentration in the liquid sample applied to the HEMT. Conventional HEMTs with the antibody immobilized in the gate region above the active channel have a high charge screening effect in high ionic strength solutions, such as serum or blood, reducing protein detection sensitivity in physiological environments where the Debye length is much smaller than the antibody.<sup>27,28</sup> The electronic double layer approaches described here do not need dilution to reduce the ionic strength.<sup>26,27</sup> It is important to point out that the ability to use a glass slide to contain the functionalized area is attractive for the

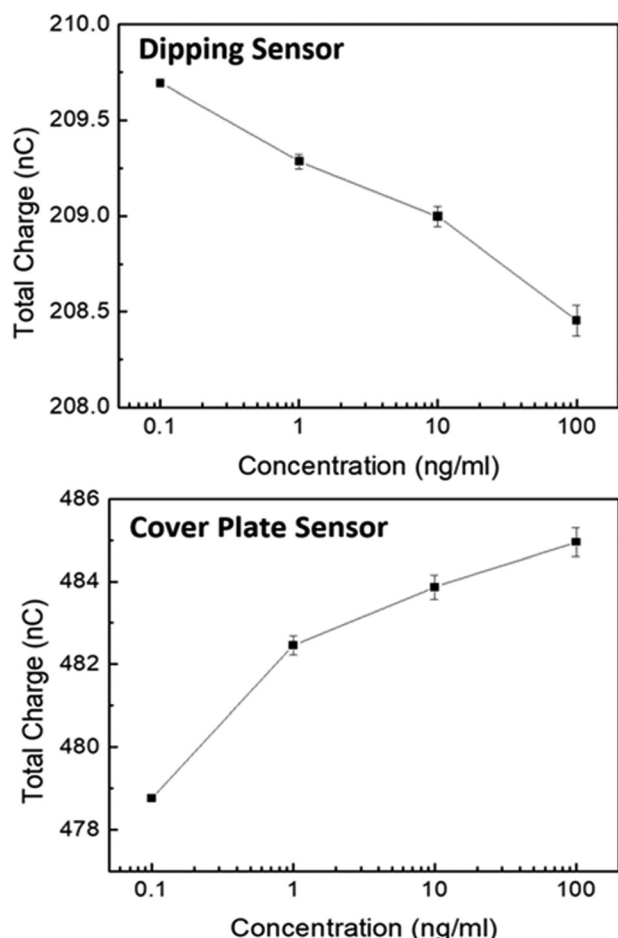


FIG. 5. The relationship of total charge to different Troponin I protein concentrations of 0.1 ng/ml, 1 ng/ml, 10 ng/ml, and 100 ng/ml in 1× PBS and 1% BSA solutions for the dipping sensor (top) or the cover glass sensor (bottom).

viewpoint of having an inexpensive, disposable cartridge approach in future sensor designs in which the HEMT itself remains as part of the electronic package.

In summary, Cardiac troponin-I (cTnI) released from damaged heart muscle is an effective biomarker for acute myocardial infarction (AMI) in terms of specificity and sensitivity, and the development of simplified, electronic-based rapid sensors is desirable. The electronic double layer HEMT designs described here enhance the current gain of the sensor in high ionic strength solutions, resulting in increased sensitivity and specificity in detection of Troponin I. The ability to use a simple, functionalized glass slide as the active sensing area opens up the possibility of inexpensive cartridge sensor designs.

The work at UF was partially supported by a Grant from the NSF I/UCRC of the Multi-functional Integrated System Technology (MIST Center) IIP-1439644. The authors acknowledge the use of the Nanoscale Research Facility (NRF) in the Nanoscience Institute for Medical and Engineering Technology at the University of Florida. The work at National Tsing Hua University was partially supported by research grants from the Ministry of Science and Technology (MOST 104-2221-E-007-142-MY3) and National Tsing Hua University (106N523CE1). The work at Dankook University was supported by the Basic Science Research Program of the National Research Foundation of Korea (NRF) funded by

the Ministry of Education (2015R1D1A1A01058663) and the Nano Material Technology Development Program through the National Research Foundation of Korea (NRF) funded by the Ministry of Science, ICT and Future Planning (2015M3A7B7045185). The work at NRL was partially supported by the Office of Naval Research.

- <sup>1</sup>S. Mythili and N. Malathi, *Biomed. Rep.* **3**, 743 (2015).
- <sup>2</sup>Z. Shimoni, R. Arbuzo, and P. Froom, *Am. J. Med.* **130**, 1205 (2017).
- <sup>3</sup>K. R. Davies, A. W. Gelb, P. H. Manninen, D. R. Boughner, and D. Bisnaire, *Br. J. Anaesth.* **67**, 58 (1991).
- <sup>4</sup>B. E. Amundson and F. S. Apple, *Clin. Chem. Lab. Med.* **53**, 665 (2014).
- <sup>5</sup>S. Korff, H. A. Katus, and E. Giannitsis, *Heart* **92**, 987 (2006).
- <sup>6</sup>B. Cummins, M. L. Auckland, and P. Cummins, *Am. Heart J.* **113**, 1333 (1987).
- <sup>7</sup>F. S. Apple, A. Falahati, P. R. Paulsen, E. A. Miller, and S. W. Sharkey, *Clin. Chem.* **43**, 2047 (1997).
- <sup>8</sup>K. Thygesen, J. S. Alpert, A. Jaffe, M. L. Simoons, B. R. Chaitma, and H. D. White, *J. Am. Coll. Cardiol.* **60**, 1581 (2012).
- <sup>9</sup>M. Zaninotto, S. Altinier, M. Lachin, P. Carraro, and M. Plebani, *Clin. Chem.* **42**, 1460 (1996).
- <sup>10</sup>T. Keller, T. Zeller, D. Peetz, S. Tzikas, A. Roth, E. Czyz, C. Bickel, S. Baldus, A. Warnholtz, M. Fröhlich, C. R. Sinning, M. S. Eleftheriadis, P. S. Wild, R. B. Schnabel, F. Lubos, N. Jachmann, S. Genth-Zotz, F. Post, V. Nicaud, L. Tiret, K. J. Lackner, T. F. Münzel, and S. Blankenberg, *N. Engl. J. Med.* **361**, 868 (2009).
- <sup>11</sup>H. Jo, H. Gu, W. Jeon, H. Youn, J. Her, S.-K. Kim, J. Lee, J. H. Shin, and C. Ban, *Anal. Chem.* **87**, 9869 (2015).
- <sup>12</sup>S. Takahashi and J. Anzai, *Materials* **6**, 5742 (2013).
- <sup>13</sup>Q. Guo, T. Kong, R. Su, Q. Zhang, and G. Cheng, *Appl. Phys. Lett.* **101**, 093704 (2012).
- <sup>14</sup>B. McDonnell, S. Hearty, P. Leonard, and R. O. Kennedy, *Clin. Biochem.* **42**, 549 (2009).
- <sup>15</sup>V. Palamalai, M. M. Murakami, and F. S. Apple, *Clin. Biochem.* **46**, 1631 (2013).
- <sup>16</sup>D. B. Diercks, W. F. Peacock, J. E. Hollander, A. J. Singer, R. Birkhahn, N. Shapiro, T. Glynn, R. Nowack, B. Safdar, C. D. Miller, E. Lewandrowski, and J. T. Nagurny, *Am. Heart J.* **163**, 74 (2012).
- <sup>17</sup>A. S. V. Shah, A. Anand, Y. Sandoval, K. K. Lee, S. W. Smith, P. D. Adamson, A. R. Chapman, T. Langdon, D. Sandeman, A. Vaswani, F. E. Strachan, A. Ferry, A. G. Stirzaker, A. Reid, A. J. Gray, P. O. Collinson, D. A. McAllister, F. S. Apple, D. E. Newby, and N. L. Mills, *Lancet* **386**, 2481 (2015).
- <sup>18</sup>B. S. Kang, H. T. Wang, F. Ren, and S. J. Pearton, *J. Appl. Phys.* **104**, 031101 (2008).
- <sup>19</sup>A. Nehra and K. P. Singh, *Biosens. Bioelectron.* **74**, 731 (2015).
- <sup>20</sup>Y.-W. Kang, G.-Y. Lee, J.-I. Chyi, C.-P. Hsu, Y.-R. Hsu, C.-H. Hsu, Y.-F. Huang, Y.-C. Sun, C.-C. Chen, S. C. Hung, F. Ren, J. A. Yeh, and Y.-L. Wang, *Appl. Phys. Lett.* **102**, 173704 (2013).
- <sup>21</sup>C.-P. Hsu, P.-C. Chen, A. K. Pulikkathodi, Y.-H. Hsiao, C.-C. Chen, and Y.-L. Wang, *ECS J. Solid State Sci. Technol.* **6**, Q63 (2017).
- <sup>22</sup>J. K. Y. Law, A. Susloparova, X. T. Vu, X. Zhou, F. Hempel, B. Qu, M. Hoth, and S. Ingebradt, *Biosens. Bioelectron.* **67**, 170 (2015).
- <sup>23</sup>D. Sarkar, W. Liu, X. Xie, C. Aaron, A. C. Anselmo, S. Mitragotri, and K. Banerjee, *ACS Nano* **8**, 3992 (2014).
- <sup>24</sup>S. Wustoni, S. Hideshima, S. Kuroiwa, T. Nakanishi, M. Hashimoto, Y. Mori, and T. Osaka, *Biosens. Bioelectron.* **67**, 256 (2015).
- <sup>25</sup>H. H. Lee, M. Bae, S.-H. Jo, J.-K. Shin, D. H. Son, C.-H. Won, and J.-H. Lee, *Sens. Actuators, B* **234**, 316 (2016).
- <sup>26</sup>I. Sarangadharan, A. Regmi, Y.-W. Chen, C.-P. Hsu, P.-c. Chen, W.-H. Chang, G.-Y. Lee, J.-I. Chyi, S.-C. Shiesh, G.-B. Lee, and Y.-L. Wang, *Biosens. Bioelectron.* **100**, 282 (2018).
- <sup>27</sup>C.-H. Chu, I. Sarangadharan, A. Regmi, Y.-W. Chen, C.-P. Hsu, W.-H. Chang, G.-Y. Lee, J.-I. Chyi, C.-C. Chen, S.-C. Shiesh, G.-B. Lee, and Y.-L. Wang, *Sci. Rep.* **7**, 5256 (2017).
- <sup>28</sup>C.-P. Hsu, Y.-F. Huang, and Y.-L. Wang, *ECS J. Solid State Sci. Technol.* **5**, Q149 (2016).
- <sup>29</sup>B. S. Kang, S. J. Pearton, J. J. Chen, F. Ren, J. W. Johnson, R. J. Therrien, P. Rajagopal, J. C. Roberts, E. L. Piner, and K. J. Linthicum, *Appl. Phys. Lett.* **89**, 122102 (2006).
- <sup>30</sup>B. S. Kang, F. Ren, M. C. Kang, C. Lofton, W. Tan, S. J. Pearton, A. Dabiran, A. Osinsky, and P. P. Chow, *Appl. Phys. Lett.* **86**, 173502 (2005).